



**HAL**  
open science

## **Scleromatobacter humisilvae gen. nov., sp. nov., a novel bacterium isolated from oak forest soil**

Sophie Mieszkin, Blandine Trouche, Julien Ancousture, Youssef Raouf,  
Stéphane Uroz, Karine Alain

### ► To cite this version:

Sophie Mieszkin, Blandine Trouche, Julien Ancousture, Youssef Raouf, Stéphane Uroz, et al.. Scleromatobacter humisilvae gen. nov., sp. nov., a novel bacterium isolated from oak forest soil. International Journal of Systematic and Evolutionary Microbiology, 2023, 73 (3), pp.005793. 10.1099/ijsem.0.005793 . hal-04236566

**HAL Id: hal-04236566**

**<https://hal.science/hal-04236566>**

Submitted on 11 Oct 2023

**HAL** is a multi-disciplinary open access archive for the deposit and dissemination of scientific research documents, whether they are published or not. The documents may come from teaching and research institutions in France or abroad, or from public or private research centers.

L'archive ouverte pluridisciplinaire **HAL**, est destinée au dépôt et à la diffusion de documents scientifiques de niveau recherche, publiés ou non, émanant des établissements d'enseignement et de recherche français ou étrangers, des laboratoires publics ou privés.

1 ***Scleromatobacter humisilvae* gen. nov., sp. nov., a novel bacterium isolated**  
2 **from an oak forest soil**

3

4 Sophie Mieszkin<sup>1,2\*</sup>, Blandine Trouche<sup>1</sup>, Julien Ancousture<sup>1</sup>, Youssef Raouf<sup>1</sup>,  
5 Stéphane Uroz<sup>2</sup> and Karine Alain<sup>1</sup>

6

7 **Author affiliations :**

8 <sup>1</sup>Univ Brest, CNRS, Ifremer, UMR6197 Biologie et Ecologie des Ecosystèmes marins  
9 Profonds, F-29280 Plouzané, France

10 <sup>2</sup>Centre INRAE-Grand Est-Nancy, Université de Lorraine, INRAE, UMR IAM, 54280  
11 Champenoux, F-54000 Nancy, France

12

13 \* **Correspondence:** Sophie.Mieszkin@univ-brest.fr

14

15 **Keywords:** *Scleromatobacter humisilvae*; *Betaproteobacteria*; *Burkholderiales*;  
16 *Comamonadaceae*; oak forest soil

17

18 **Repositories:**

19 The 16S rRNA gene sequence and the assembled genome sequences of strain BS-  
20 T2-15<sup>T</sup> have been deposited in GenBank under the accession numbers OM630150  
21 and JAJLJH000000000, respectively.

22

23 **Abbreviations:**

24 AAI, Average Amino acids Identity; AF, Alignment Fraction; ANI, Average Nucleotide  
25 Identity; CAPSO, N-cyclohexyl-3-aminopropanesulfonic acid; COGs, cluster of

26 orthologous groups; dDDH, Digital DNA-DNA hybridization; DMSO, dimethyl  
27 sulfoxide; DPG, diphosphatidylglycerol; DSMZ, Deutsche Sammlung von  
28 Mikroorganismen und Zellkulturen; HEPES, 4-(2-hydroxyethyl)-1-  
29 piperazineethanesulfonic acid; HOMOPIPES, Homopiperazine-1,4-bis(2-  
30 ethanesulfonic acid); HPIC, High Pressure Ion Chromatography; ICSP, International  
31 Committee on Systematics of Prokaryotes; KEGG, Kyoto Encyclopedia of Genes and  
32 Genomes; MES, 2-(N-Morpholino) EthaneSulfonic acid; MMN, Mannitol-Mobility-  
33 Nitrate agar medium; OGRI, overall genome related indices; PE,  
34 Phosphatidylethanolamine; PG, Phosphatidylglycerol; PHA, Polyhydroxyalkanoates;  
35 PIPES, Piperazine-N,N'-bis(2-ethanesulfonic acid); POCP, Percentage Of Conserved  
36 Proteins; TEM, Transmission Electron Microscopy; TSA, Tryptic Soy Agar; TSB,  
37 Tryptic Soy Broth; UBOCC, UBO Culture Collection.

38 **Abstract**

39 A novel bacterial strain, designated BS-T2-15<sup>T</sup>, isolated from forest soil in close  
40 proximity to decaying oak wood, was characterized using a polyphasic taxonomic  
41 approach. Phylogenetic analyses based on 16S rRNA gene sequences as well as  
42 phylogenomic analyses based on coding sequences of 340 concatenated core  
43 proteins indicated that strain BS-T2-15<sup>T</sup> forms a distinct and robust lineage in the  
44 *Rubrivivax-Roseateles-Leptothrix-Azohydromonas-Aquincola-Ideonella* branch of the  
45 order *Burkholderiales*. The amino acid identity (AAI) and the percentage of  
46 conserved proteins (POCP) between genome of strain BS-T2-15<sup>T</sup> and genomes of  
47 closely related type strains ranged from 54.27 to 66.57% and from 43.17 to 49.27%,  
48 respectively, providing genomic evidence that strain BS-T2-15<sup>T</sup> represents a new  
49 genus. Its cells stain Gram-negative, are aerobic, motile by a polar flagellum, rod-  
50 shaped and form incrustated white to ivory colonies. Optimal growth is observed at 20-  
51 22°C, pH 6 and 0% NaCl. The predominant fatty acids of strain BS-T2-15<sup>T</sup> are C<sub>16:1</sub>  
52  $\omega$ 7c, C<sub>16:0</sub> and C<sub>14:0</sub> 2-OH. Its polar lipid profile consists of a mixture of  
53 phosphatidylethanolamine, diphosphatidylglycerol and phosphatidylglycerol and its  
54 main respiratory quinone is ubiquinone 8. The estimated size of its genome is 6.28  
55 Mb with a DNA G+C content of 69.56 mol%. Therefore, on the basis of phenotypic  
56 and genotypic properties, the new strain BS-T2-15<sup>T</sup> represents a new genus and a  
57 novel species for which the name *Scleromatobacter humisilvae* gen. nov., sp. nov., is  
58 proposed. The type strain is BS-T2-15<sup>T</sup> (DSM 113115<sup>T</sup> =UBOCC-M-3373<sup>T</sup>).

59 In forest ecosystems, wood decay is an important process that participates to the soil  
60 fertility through the action of a complex guild of decomposers [1, 2]. Among them,  
61 fungi are considered as the main actors, while the role of bacteria is much less  
62 documented [3]. To fill this gap, the taxonomic diversity and the metabolic and  
63 functional potential of bacterial strains isolated from a soil-decaying-wood continuum  
64 have been investigated [4]. Overall, this study demonstrated a community dominated  
65 by representatives of the genera *Paraburkholderia* (*Betaproteobacteria*),  
66 *Streptomyces*, *Kitasatospora*, *Arthrobacter* and *Streptacidiphilus* (*Actinobacteria*),  
67 *Dyella* (*Gammaproteobacteria*) and by uncharacterized bacterial strains [4]. At the  
68 functional level, this study also revealed that soil bacterial communities have the  
69 potential to decompose organic matter and a stronger effectiveness than those  
70 isolated from decaying oak wood. The taxonomic assignation and functional  
71 screening allowed the identification of various strains of interest, among which strain  
72 BS-T2-15<sup>T</sup>, one of the uncharacterized strains, was selected to be further  
73 characterized in the present study to clarify its taxonomic position within the  
74 *Rubrivivax-Roseateles-Leptothrix-Azohydromonas-Aquincola-Ideonella* branch of the  
75 order *Burkholderiales*, in the class *Betaproteobacteria*. To date, there is a taxonomic  
76 uncertainty regarding the classification of these genera at the family rank level.  
77 Recently, Liu *et al.* [5] proposed to refer to this branch as the closest-to-  
78 *Comamonadaceae* (CTC) group, as it forms a phylogenetically coherent group close  
79 to genera belonging to the *Comamonadaceae* family. They proposed to classify the  
80 CTC group as a new family, 'Sphaerotilaceae' fam. nov., based on phylogenomic  
81 analyses, genome relatedness indices and phenotypic data. However, this new  
82 delineation is not yet recognized by the International Committee on Systematics of  
83 Prokaryotes (ICSP). In addition, they also proposed several taxonomic revisions at

84 the genera and species levels. Among remarkable physiological features of the  
85 *Rubrivivax-Roseateles-Leptothrix-Azohydromonas-Aquincola-Ideonella* branch, some  
86 species are known to be involved in the biodegradation of petroleum compounds or  
87 in the reduction of chlorate to chloride under anaerobic conditions [6-8].

88 In the present study, we performed a polyphasic taxonomic characterization of strain  
89 BS-T2-15<sup>T</sup> and provided phenotypic, phylogenomic, and genomic evidences that it  
90 meets the criteria for delineating a new species of a new genus within the *Rubrivivax-*  
91 *Roseateles-Leptothrix-Azohydromonas-Aquincola-Ideonella* branch. We propose to  
92 name this new species *Scleromatobacter humisilvae* gen. nov., sp. nov.

93

#### 94 **ISOLATION AND ECOLOGY**

95 Strain BS-T2-15<sup>T</sup> is from a collection of 308 bacterial strains established as part of a  
96 study on the functional abilities of bacterial isolates from decaying wood and their  
97 comparison with the properties of bacteria from underlying soil [4]. The experimental  
98 set up consisted in oak discs that have been placed during 9 months on the soil  
99 surface of the forest experimental site of Champenoux (north-eastern France; Lat:  
100 48.718420° N; Long: 6.346580° E; Alt: 248 m; 0.5 ha of surface). Strain BS-T2-15<sup>T</sup>  
101 was isolated from the bulk soil in direct contact with decaying oak disc by serial  
102 dilutions on 1/10 diluted Tryptic Soy Agar (TSA) medium (Difco's Tryptic Soy Broth  
103 (TSB) 3 g.L<sup>-1</sup> and agar 15 g.L<sup>-1</sup>) containing cycloheximide (100 g.L<sup>-1</sup>, final  
104 concentration), with a pH adjusted to 5. The strain was then purified by 3 successive  
105 spreads on 1/10 diluted TSA plates at pH 5 to obtain a pure culture. The strain BS-  
106 T2-15<sup>T</sup> was then grown routinely on 1/10 TSA or 1/10 TSB media adjusted to pH 5  
107 during 3 days at 20°C, under agitation (250 rpm). Its purity was routinely confirmed

108 by microscopic observations, and by sequencing of its 16S rRNA gene and genome.  
109 Stock cultures were stored at  $-80^{\circ}\text{C}$  in 1/10 TSB medium supplemented with 5%  
110 (v/v) dimethylsulfoxide (DMSO). Main chemical characteristics of the bulk soil  
111 samples were  $\text{pH } 4.65 \pm 0.10$ ,  $48.38 \pm 7.93 \text{ g.kg}^{-1}$  total carbon,  $3.26 \pm 0.49 \text{ g.kg}^{-1}$   
112 total nitrogen,  $0.17 \pm 0.01 \text{ g.kg}^{-1}$  phosphorus extracted according to the Duchaufour  
113 method and  $83.80 \pm 13.92 \text{ g.kg}^{-1}$  organic matter [4].

114 Strain BS-T2-15<sup>T</sup> (DSM 113115<sup>T</sup> = UBOCC-M-3373<sup>T</sup>) is available in the public culture  
115 collections Deutsche Sammlung von Mikroorganismen und Zellkulturen (DSMZ;  
116 <https://www.dsmz.de/collection>) and UBO Culture Collection (UBOCC;  
117 <https://www.univ-brest.fr/ubocc>).

118

## 119 **MORPHOLOGY AND PHYSIOLOGY**

120 Colony morphology of the isolate BS-T2-15<sup>T</sup> was observed on 1/10 TSA adjusted to  
121 pH 6. Cell morphology and motility were determined by light microscopy (Olympus  
122 BX60 and CX40) and transmission electron microscopy (TEM; JEOL JEM 1400).  
123 Motility was also observed by using the Mannitol-Motility-Nitrate agar medium (MMN,  
124 composed (per liter) of 10 g tryptic hydrolysate of casein, 1 g potassium nitrate, 7.5 g  
125 mannitol, 40 mg phenol red and 3.5 g agar), which was also used to evidence  
126 mannitol fermentation and nitrate reductase activity. Gram-staining was determined  
127 using standard procedures and confirmed with a KOH (3%) test. Catalase and  
128 cytochrome oxidase activities were respectively evaluated using  $\text{H}_2\text{O}_2$  and strips of  
129 N, N, N',N'-tetramethyl-*p*-phenylenediamine dihydrochloride (Bio-Rad). The oxidase  
130 test was repeated several times using independent cultures to confirm the result.  
131 Colonies of BS-T2-15<sup>T</sup> are circular and rough with a color between white and ivory. A  
132 major phenotypic feature is that its colonies are incrustated in the agar medium. To our

133 knowledge, this was not yet reported in the literature for genera belonging to the  
134 *Rubrivivax-Roseateles-Leptothrix-Azohydromonas-Aquicola-Ideonella* branch. Cells  
135 are Gram-negative coccobacilli that divide by binary fission and occur mainly singly,  
136 but can also form aggregates (Fig. 1A, B). Cell size range from 0.59 to 0.93  $\mu\text{m}$  wide  
137 (mean 0.78  $\mu\text{m}$ ;  $n=45$ ) and from 1.71 to 2.73  $\mu\text{m}$  long (mean 2.15  $\mu\text{m}$ ;  $n=45$ ). Strain  
138 BS-T2-15<sup>T</sup> is motile, as confirmed by growth observations on MMN agar medium and  
139 the observation of a single polar flagellum per cell by TEM (Fig. 1C, D). Refrigent  
140 intracellular granules, which could be polyhydroxyalkanoates (PHA) storage  
141 granules, were also observed (Fig. 1A). The strain is catalase positive and oxidase  
142 negative. The latter phenotypic feature clearly distinguishes strain BS-T2-15<sup>T</sup> from  
143 other genera of the *Rubrivivax-Roseateles-Leptothrix-Azohydromonas-Aquicola-*  
144 *Ideonella* branch which are all oxidase positive. However, it is important to note that,  
145 cytochrome C oxidase complex was identified in its genome. This point is discussed  
146 latter in the study.

147

148 Physiological characterization of the novel strain BS-T2-15<sup>T</sup> was carried out  
149 aerobically, in triplicate, on 1/10 TSA or TSB adjusted to pH 6 at 20°C and under  
150 agitation (250 rpm). Determination of the temperature range for growth and salt  
151 tolerance were respectively tested over the range 0-45°C, at 5°C intervals and 0-10%  
152 NaCl (w/v), at 0.5% intervals, both for 10 days on 1/10 TSA at pH 6. Growth was  
153 observed from 4 to 30°C with optimal growth between 20-22°C. Concerning salt  
154 tolerance, the strain grew only at 0.5% NaCl and exhibited an optimal growth without  
155 sodium chloride. The pH range for growth was tested from pH 2.0 to pH 12 (at 20°C),  
156 with increments of 1 unit on 1/10 TSB medium for 8 days. Cells were routinely  
157 enumerated by direct cell counting using a modified Thoma chamber (Preciss,



158 France; surface: 0.0025 mm<sup>2</sup>, depth: 10 µm). The following buffers (each at 20 mM,  
159 Sigma-Aldrich, Darmstadt, Germany) were used to adjust the required pH: pH 4.0  
160 and 5.0 with HOMOPIPES buffer, pH 6.0 with MES buffer, pH 7.0 with PIPES buffer,  
161 pH 8.0 with HEPES buffer, and pH 9.0 and 10.0 with CAPSO buffer. For pH 2.0, 3.0,  
162 11.0 and 12.0, no buffer was used. Growth of strain BS-T2-15<sup>T</sup> was observed from  
163 pH 2.0 to 12 with optimal growth at pH 6. The growth kinetics of BS-T2-15<sup>T</sup> under  
164 optimal conditions was then studied in triplicates, on 1/10 TSB adjusted to pH 6 at  
165 22°C with no NaCl salt, under agitation (250 rpm) for 4 days. Cell growth was  
166 monitored by direct cell counting, every 3 h using a modified Thoma chamber, in  
167 order to determine the growth rate and doubling time of the strain under optimal  
168 culture conditions. The growth rate and the generation time of strain BS-T2-15<sup>T</sup> are  
169 respectively, 0.17 h<sup>-1</sup> and 3 h 58 min.

170

171 Utilization of carbon sources was investigated using the mineral basis of the 1/10  
172 TSB medium containing (L<sup>-1</sup>): 0.25 g KH<sub>2</sub>PO<sub>4</sub> and adjusted at pH 6. Each substrate  
173 (lactose, *D*-mannose, *D*-ribose, *D*-maltose, *D*-glucose, *N*-acetylglucosamine, butyric  
174 acid, gluconate, citrate, benzoate, acetate, pyruvate and urea) was supplied at a final  
175 concentration of 20 mM. Utilization of nitrogen sources was investigated using 1/10  
176 TSB medium adjusted at pH 6 with nitrate and ammonium supplied at a final  
177 concentration of 20 mM, while nitrite was supplied at a final concentration of 5 mM.  
178 Before inoculation, cells at the end of their exponential growth phase were harvested  
179 and washed three times with distilled water and then the bacterial suspension was  
180 adjusted to obtain a Mac Farland index value of 1. A medium composed of mineral  
181 basis of the 1/10 TSB without carbon source was used as negative control for each  
182 carbon utilization bioassay and a positive control was performed using 1/10 TSB

183 medium adjusted at pH 6. The hydrolysis of cellulose was determined using  
184 Carboxymethyl Cellulose (CM Cellulose) as described by Mieszkin *et al.* [4]. These  
185 tests were completed with liquid or solid cultures allowing to determine: (i) mannitol  
186 fermentation and presence of nitrate reductase (MMN agar medium), (ii) fermentative  
187 pathways (mixed acids or butane-2,3-diol pathways; Clark and Lubs liquid medium),  
188 (iii) glucose and lactose fermentation, gas and H<sub>2</sub>S production (Kligler-Hajna agar  
189 medium), and, (iv) citrate utilization (Simmons citrate agar medium). For these  
190 assays, culture media, cell cultures and washes and preparation of bacterial  
191 suspensions were performed as described above and by Mieszkin *et al.* [9]. Strain  
192 BS-T2-15<sup>T</sup> is chemoorganoheterotrophic and grows by aerobic respiration. It  
193 catabolizes *D*-glucose, lactose and pyruvate while a moderate growth was obtained  
194 with *D*-ribose, *N*-acetylglucosamine, urea and gluconate. A weak growth was also  
195 observed with all the nitrogen substrates tested (nitrate, nitrite and ammonium). In  
196 addition, BS-T2-15<sup>T</sup> is capable of using nitrate or nitrite as terminal electron  
197 acceptors showing that the nitrate reductase is functional (Table 1).

198

199 Volatile fatty acid production of strain BS-T2-15<sup>T</sup> after growth in duplicate in 1/10 TSB  
200 was assessed by high-pressure ion chromatography (Dionex ICS-6000 HPIC)  
201 (Growth conditions: pH 6, 20°C, under agitation (250 rpm), for 3 days). HPIC  
202 analyses showed that the strain consumed all the pyruvate present in the medium  
203 during its growth (approximately 930 μM), but did not produce acetate, lactate,  
204 pyruvate or oxalate under these culture conditions. This is consistent with previous  
205 results showing that it is capable to grow with pyruvate as sole carbon source.

206 Strain BS-T2-15<sup>T</sup> was not capable to use chlorate as sole terminal electron acceptor  
207 (at 20 mM), when grown anaerobically on 5 g.L<sup>-1</sup> NaCl, with 1 g.L<sup>-1</sup> tryptone as  
208 carbon and energy source (with respect to negative and positive controls).

209 Sensitivity to antibiotics of strain BS-T2-15<sup>T</sup> was tested by the disc diffusion method  
210 after spreading cell suspensions (1 McFarland) on 1/10 TSA adjusted to pH 6 at  
211 20°C for 7 days. Discs were impregnated with antibiotic solutions to obtain a final  
212 quantity of antibiotic per disc of: kanamycin (40µg), rifampicin (30 µg), novobiocin (30  
213 µg), gentamicin (15 µg), ampicillin (10 µg), penicillin (10 U), oxacillin (5 µg),  
214 oxytetracycline (30 µg), chloramphenicol (30 µg), and streptomycin (10 µg). The  
215 discs were then placed on the agar surface. The inhibition zones were read after 3  
216 days of incubation at 20°C. Among the antibiotics tested, strain BS-T2-15<sup>T</sup> was  
217 sensitive to kanamycin, novobiocin, gentamicin and streptomycin.

218

## 219 **CHEMOTAXONOMY**

220 In order to analyze respiratory quinones, polar lipids, and fatty acids, cells of strain  
221 BS-T2-15<sup>T</sup> were cultured in 1/10 TSB pH 6 at 20°C under agitation (250 rpm) and  
222 then harvested by centrifugation (800 g; 10 min) at the end of their exponential phase  
223 of growth. These analyses were carried out by the Identification Service of the DSMZ  
224 (Braunschweig, Germany) as described by Tindall [10, 11] and Kuykendall *et al.* [12].

225 The major respiratory quinone identified for strain BS-T2-15<sup>T</sup> is ubiquinone 8 (Q-8).

226 The polar lipid profile of the novel isolate consisted in phosphatidylethanolamine  
227 (PE), diphosphatidylglycerol (DPG), and phosphatidylglycerol (PG). A common  
228 feature of the new strain and species belonging to the related genera *Leptothrix*,  
229 *Rubrivivax*, *Ideonella* and *Aquicola* is the high proportion of PE and PG, which is  
230 consistent with the *Comamonadaceae* family [13, 14]. However, a major

231 characteristic of strain BS-T2-15<sup>T</sup> is its high content of DPG, a polar lipid that is  
232 absent or only present in low proportions in the type strains of the closest genera  
233 (Table S1 et Fig. S1).

234 The predominant cellular fatty acids (>10% of the total fatty acids) of strain BS-T2-  
235 15<sup>T</sup> are C<sub>16:1</sub> ω7c (40.45%), C<sub>16:0</sub> (25.18%) and C<sub>14:0</sub> 2-OH (10.49%) (Table 2).  
236 Noticeably, the main saturated fatty acid detected (*i.e.*, C<sub>16:0</sub>) appeared dominant and  
237 common among BS-T2-15<sup>T</sup> and the four closely related genera (*Leptothrix*,  
238 *Rubrivivax*, *Ideonella* and *Aquicola*), while the hydroxyl fatty acid (*i.e.* C<sub>14:0</sub> 2-OH)  
239 was only detected in strain BS-T2-15<sup>T</sup> (Table 1). In addition, the presence of the  
240 unsaturated fatty acid C<sub>16:1</sub> ω7c is another major feature of the new strain but could  
241 also be represented by summed feature 3 (C16: 1 ω7c o and/or C16: 1 ω6c) in  
242 *Rubrivivax gelatinosus* DSM 1709<sup>T</sup> and *Ideonella dechloratans* CGUG 30977<sup>T</sup>.

243

#### 244 **16S rRNA GENE PHYLOGENY**

245 A full 16S rRNA gene sequence (1512 nt) of strain BS-T2-15<sup>T</sup> was extracted from the  
246 genome using the bacterial ribosomal predictor tseemann/barnnap on Galaxy v1.2.1  
247 [19]. Pairwise 16S rRNA gene sequence similarity was calculated using the global  
248 alignment algorithm implemented at the EzTaxon-e server ([http://eztaxon-  
249 e.ezbiocloud.net/](http://eztaxon-e.ezbiocloud.net/); [20]). Phylogenetic analyses were performed using the software  
250 Seaview version 4.7 for trees reconstruction by the neighbor-joining (NJ) and  
251 maximum parsimony (MP) methods [21-23]. The evolutionary distances were  
252 respectively calculated using the Kimura two-parameters and the Dnapars modes.  
253 The robustness of the inferred topology was assessed by bootstrap analyses based  
254 on 1,000 replications. A third tree was build using the maximum likelihood (PhyML)  
255 method with the subtree-pruning-regrafting algorithm

256 ([http://phylogeny.lirmm.fr/phylo.cgi/simple\\_phylogeny.cgi](http://phylogeny.lirmm.fr/phylo.cgi/simple_phylogeny.cgi)) [24, 25]. The 16S rRNA  
257 gene sequence analysis of strain BS-T2-15<sup>T</sup> showed that it belongs to the class  
258 *Betaproteobacteria*, the order *Burkholderiales* and the family *Comamonadaceae*. The  
259 NJ and MP phylogenetic trees based on 16S rRNA gene sequences revealed that  
260 strain BS-T2-15<sup>T</sup> does not form a monophyletic clade with any representatives of  
261 related taxa (Fig. S2 and S3). However, most of the bootstrap percentages of the  
262 trees had a very low value (<70%). Concerning the PhyML tree, a clade was  
263 obtained with strain BS-T2-15<sup>T</sup> and *Leptothrix mobilis* (Feox-1; X97071) but it was  
264 distantly related to most of the genera of the *Rubrivivax-Roseateles-Leptothrix-*  
265 *Azohydromonas-Aquincola-Ideonella* branch (Fig. S4).

266 Comparative analysis of the 16S rRNA gene sequence of the novel strain with  
267 relatives having validly published names showed that BS-T2-15<sup>T</sup> is equidistant to  
268 species belonging to the genera *Ideonella* (96.55–95.78%), *Leptothrix* (96.47–  
269 95.50%), *Aquincola* (96.47–96.13%), *Rubrivivax* (96.40–95.85%) and *Aquabacterium*  
270 (96.13-95.53%). Its closest relative is *Ideonella azotifigens* 1a22<sup>T</sup> (96.55%) followed  
271 by *Leptothrix mobilis* FeOx-1<sup>T</sup> (96.47%), *Aquincola tertiaricarbonis* L10<sup>T</sup> (96.47%),  
272 and *I. dechloratans* CCUG 30898<sup>T</sup> (96.47%), *Rubrivivax gelatinosus* ATCC 17011<sup>T</sup>  
273 (96.40%) and *R. benzoatilyticus* JA2<sup>T</sup> (96.40%).

274 Overall, these results demonstrate that the 16S rRNA gene-based phylogeny lacks of  
275 resolution to evaluate the taxonomic position of strain BS-T2-15<sup>T</sup> among the  
276 *Rubrivivax-Roseateles-Leptothrix-Azohydromonas-Aquincola-Ideonella* branch, as  
277 previously underlined by Liu *et al.* [25]. Genome based phylogeny is therefore  
278 mandatory to gain a better resolution to assign with certainty the taxonomic position  
279 of the new strain BS-T2-15<sup>T</sup>.

280

## 281 **GENOME FEATURES**

282 Genomic DNA of strain BS-T2-15<sup>T</sup> was extracted with a standard PCI (Phenol:  
283 Chloroform: Isoamyl Alcohol (25:24:1)) protocol [26]. Whole genome sequencing was  
284 performed by the Novogene company (Cambridge, United Kingdom), using the  
285 Illumina NovaSeq 6000 PE150 technology (2×150 bp paired-end reads). Reads  
286 quality was then evaluated with Fast QC (v0.11.9;  
287 <https://www.bioinformatics.babraham.ac.uk/projects/fastqc/> [27]. The whole genome  
288 was assembled by using the Shovill pipeline with SPAdes and default parameters  
289 [28]. Genome completeness and potential contamination were estimated with  
290 CheckM on the MicroScope Microbial Genome Annotation and Analysis Platform  
291 (MaGe; <https://mage.genoscope.cns.fr>) [29]. The overall genome size was 6,276,266  
292 bp (for 100% completion and 0% contamination) for 28 contigs and the GC content  
293 was 69.56%. The N50 and L50 values were respectively 579,168 bp and 3 contigs. A  
294 total of 5,712 coding DNA sequences (CDSs), 3 rRNA and 55 tRNA genes  
295 (corresponding to the 20 essential amino acids) were detected using the MaGe  
296 pipeline (Table 3 and Fig S5). Most of the CDSs (78.29%) could be assigned to at  
297 least one cluster of orthologous groups (COGs). COGs categories related to  
298 metabolic processes were dominant (38.30% of the CDSs) and the main processes  
299 involved (>5% of the CDSs) were: (i) amino acid transport and metabolism (E;  
300 9.04%); (ii) carbohydrate transport and metabolism (G; 6.45%); inorganic ion  
301 transport and metabolism (P; 5.45%) and (iv) energy production and conversion (C;  
302 5.38%). Then, 24.56% of CDSs were allocated to the COGs category related to  
303 cellular process and signaling and the following processes were dominant: signal  
304 transduction mechanisms (T; 7.64%) and cell wall, membrane and envelope

305 biogenesis (M; 5.26%). Finally, 14.91% of the CDSs were predicted to be involved in  
306 the processes dedicated to the information storage and processing (Table S2).

307

308 In addition to phylogenetic trees based on the 16S rRNA sequences that do not  
309 provide robust phylogenetic reconstructions with this dataset, a phylogenomic tree for  
310 was constructed based on 340 core gene clusters (gene clusters appearing once in  
311 each genome).

312 This tree encompassed 21 reference genomes representative of the *Rubrivivax-*  
313 *Roseateles-Leptothrix-Azohydromonas-Aquicola-Ideonella* branch and  
314 phylogenetically related to strain BS-T2-15<sup>T</sup> (*Aquabacterium commune* DSM 11901<sup>T</sup>,  
315 *Aquicola rivuli* KYPY4<sup>T</sup>, *Aquicola tertiaricarbonis* DSM 18512<sup>T</sup>, *Azohydromonas*  
316 *lata* NBRC 102462<sup>T</sup>, *Ideonella azotifigens* DSM 21438<sup>T</sup>, *Ideonella benzenivorans* B7,  
317 *Ideonella dechloratans* CGUG 30977<sup>T</sup>, *Ideonella livida* TBM-1<sup>T</sup>, *Ideonella paludis*  
318 KCTC 32238<sup>T</sup>, *Ideonella sakaiensis* 201-F6<sup>T</sup>, *Leptothrix cholodnii* SP-6<sup>T</sup>, *Leptothrix*  
319 *mobilis* DSM 10617<sup>T</sup>, *Roseateles aquatilis* CCUG 48205<sup>T</sup>, *Roseateles depolymerans*  
320 KCTC 42856<sup>T</sup>, *Rubrivivax albus* ICH-3<sup>T</sup>, *Rubrivivax benzoatilyticus* JA2<sup>T</sup>, *Rubrivivax*  
321 *gelatinosus* DSM 1709<sup>T</sup>, *Schlegelella brevitalea* DSM 7029<sup>T</sup>, *Sphaerotilus hippei*  
322 DSM 566<sup>T</sup>, *Sphaerotilus natans* ATCC 13338<sup>T</sup> and *Sphaerotilus natans* subsp.  
323 *sulfidivorans* D-507<sup>T</sup>), the target genome BS-T2-15<sup>T</sup> and two closely related  
324 Metagenome Assembled Genomes (MAGs; from the Genome Taxonomy Database  
325 (GTDB, <https://gtdb.ecogenomic.org/>); accession numbers GB\_GCA\_013289985.1  
326 and GB\_GCA\_903845345.1) artificially classified as genus CAIMXF01. These  
327 closely related MAGs were respectively recovered from a forest soil [30] and from  
328 stratified freshwater lakes and ponds [31-33]. The phylogenomic tree was built as  
329 follows: (i) amino acid sequences were extracted, aligned and concatenated using

330 command line *anvi-get-sequences-for-gene-clusters* on Anvi'o v. 7.1 [34], then (ii)  
331 positions with over 0.5 gap frequency were masked, and finally (iii) a maximum  
332 likelihood tree was computed using IQTREE (v2.0.3, [35, 36]) under the model WAG  
333 with 1,000 ultrafast bootstrap replicates (See SI for more details). The tree was  
334 rooted using the genome of *Alcaligenes faecalis* ZD02 (GCA\_000967305.2) as an  
335 outgroup. A second phylogenomic tree was built by placing BS-T2-15<sup>T</sup> in the GTDB  
336 tree using GTDB-tk (v2.1, [37]), then subsetting the tree to family *Burkholderiaceae*  
337 and genus *Escherichia*, extracting the amino acid alignment, masking positions with  
338 over 0.5 gap and computing a maximum likelihood (ML) tree with IQTREE under the  
339 model WAG as described above. This second tree was built with 229 MAGs and 60  
340 cultivated bacterial strains from the *Rubrivivax-Roseateles-Leptothrix-*  
341 *Azohydromonas-Aquincola-Ideonella* branch.

342 The phylogenomic tree built with the 21 reference genomes and the two MAGs  
343 closely related to strain BS-T2-15<sup>T</sup>, was very robust with high ultrafast bootstrap  
344 values, and showed a distinctly deeper branching of strain BS-T2-15<sup>T</sup> with its two  
345 closely related MAGs and a close proximity to the *Ideonella* clade (Fig. 2). A similar  
346 result was also obtained with the phylogenomic tree built with the 229 MAGs (Fig.  
347 S6). Therefore, these two phylogenomic trees indicate that strain BS-T2-15<sup>T</sup> indeed  
348 represents a new genus of the *Comamonadaceae* family within the order  
349 *Burkholderiales*, and belongs to the *Rubrivivax-Roseateles-Leptothrix-*  
350 *Azohydromonas-Aquincola-Ideonella* branch.

351  
352 In addition to the phylogenomic trees, Overall Genome Related Indices (OGRI) were  
353 obtained by pairwise calculations between genome of strain BS-T2-15<sup>T</sup>, the two  
354 closely related MAGs of strain BS-T2-15<sup>T</sup> and the 21 reference genomes. The



355 average nucleotide identity scores (ANI) were obtained using the FastANI calculator  
356 tool from the GTDB web server (<https://gtdb.ecogenomic.org/tools/fastani>) [39]. In  
357 addition, FastANI calculator provided also the alignment fraction (AF) values between  
358 genomes. Digital DNA-DNA hybridization (dDDH) scores were determined by the  
359 genome-to-genome distance calculator (GGDC 2.1), using formula 2 [40]. The  
360 average amino acid identity (AAI) calculations between genomes were determined as  
361 described by Kim *et al.* [41] using the EzAAI pipeline (<http://leb.snu.ac.kr/ezaai>). The  
362 percentage of conserved proteins (POCP) was estimated as described by Qin *et al.*  
363 [42].

364 Digital DNA-DNA hybridization and ANI values between the strain BS-T2-15<sup>T</sup>  
365 genome and the genomes of type strains of the closest genera ranged from 20.00 to  
366 20.50% and from 78.50 to 79.70%, respectively (Table 3). These values are both far  
367 below the dDDH threshold level of 70% and the ANI value of 95-96% that are  
368 generally accepted for species delineation [43, 44]. Concerning the AAI and POCP  
369 values between genome of strain BS-T2-15<sup>T</sup> and genomes of the type strains of the  
370 closest genera, they ranged, respectively, from 64.27 to 66.57% and from 43.17 to  
371 49.27% (Table 3). AAI values are close to the 65% cutoff value generally accepted  
372 for delineating a new genus, while POCP values are below the 50% threshold  
373 recognized for demarcating a new genus [42, 45]. Finally, the AF values ranged  
374 between 0.40 and 0.48 between genomes of strain BS-T2-15<sup>T</sup> and type strains of the  
375 closest genera (Table 3), and were observed in conjunction with low ANI values [46],  
376 which is not incompatible with the description of a new genus. In this case, POCP  
377 and, to a lesser extent, ANI, are the most relevant indices to demonstrate that strain  
378 BS-T2-15<sup>T</sup> represents a new genus. Similar results were obtained when considering  
379 the 21 reference genomes (Fig. S7 and Tab. S3). In addition, all OGR1 values

380 obtained between the BS-T2-15<sup>T</sup> strain genome and the genomes of its two closely  
381 related MAGs were higher compared to the values obtained against genomes of  
382 cultured type strains. These OGRI values relative to the closest MAGs were  
383 respectively in the range of 30.10-40.40% and 87.40-88.90% for dDDH and ANI, and  
384 in the range of 84.14-86.43%, 70.43-74.76% and 0.70-0.80 for AAI, POCP and AF  
385 indices (Tab S4-S8). These dDDH and ANI values are below the threshold accepted  
386 for species delineation while the AAI, POCP and AF values are above the threshold  
387 for a new genus delineation. Overall, these OGRI analyses clearly show that strain  
388 BS-T2-15<sup>T</sup> and its two closely related MAGs (i) belong to the same genus, (ii)  
389 represent a new genus of the *Rubrivivax-Roseateles-Leptothrix-Azohydromonas-*  
390 *Aquicola-Ideonella* branch and, (iii) belong to three distinct genomic species.  
391 Furthermore, values of the different OGRI indices calculated between the species of  
392 the genus *Ideonella* and strain BS-T2-15<sup>T</sup> and its two closely related MAGs are much  
393 lower than those obtained between strain BS-T2-15<sup>T</sup> and its two closely related  
394 MAGs (Tab S4-S8). Thus, OGRI indices, as well as phylogenomic analyses, lead all  
395 to the conclusion that strain BS-T2-15<sup>T</sup> represents a new species of a new genus of  
396 the *Rubrivivax-Roseateles-Leptothrix-Azohydromonas-Aquicola-Ideonella* branch.

397

398 For gene function prediction, genome annotations were performed with the MaGe  
399 platform using KEGG and BioCyc databases. The genome of the new strain BS-T2-  
400 15<sup>T</sup> encodes metabolic pathways for organoheterotrophic growth. Notably, the  
401 genome encodes a complete pentose phosphate pathway, and a complete Entner-  
402 Doudoroff pathway. The tricarboxylic acid cycle (TCA) pathway for aerobic  
403 respiration is almost complete (one enzyme missing). The genome of the novel  
404 isolate encodes also the nitrate VIII reduction pathway (dissimilatory) for anaerobic

405 nitrate respiration, which has been shown to be functional experimentally.  
406 Degradation pathways for organic compounds such as amino acids (alanine,  
407 arginine, asparagine, serine, glutamine, glycine, histidine, cysteine, lysine, ornithine,  
408 taurine, threonine and tryptophan), carbohydrates (acetoin, chitin, glucose, glucose-  
409 1-phosphate, lactose, ribose and xylose), aromatic compounds (anthranilate,  
410 gentisate, phenylacetate and protocatechuate), alcohols (ethanol and glycerol),  
411 aldehyde (L-lactaldehyde), amines and polyamines (choline, 4-aminobutyrate,  
412 ethanolamine and urea), and carboxylates (D-gluconate, glutaryl CoA, glycolate and  
413 glyoxylate) are evidenced. The cytochrome C oxidase complex (EC number: 7.1.1.9;  
414 locus tags: COMBST215\_v1\_20371; 20374; 20375; 20376; 80152; 80156; 80157)  
415 was also identified despite that the oxidase activity not being demonstrated  
416 experimentally. The cyclopropane fatty acid (CFA) biosynthesis *via* the cyclopropane-  
417 fatty-acyl-phospholipid synthase (EC number: 2.1.1.79; locus tag:  
418 COMBST215\_v1\_10589; 50189) and the arginine dependent acid resistance  
419 (arginine decarboxylase; EC number: 4.1.1.19; locus tag: COMBST215\_v1\_10270)  
420 pathways are present and may give the strain a competitive advantage in acidic  
421 environments such as the forest soil ecosystem. The new strain BS-T2-15<sup>T</sup> has also  
422 the genetic potential to detoxify arsenate using glutaredoxin (gene: *arsC*; EC number:  
423 1.20.4.1; locus tag: COMBST215\_v1\_40055) and to degrade superoxide radicals  
424 (identification of superoxide dismutase (EC number: 1.15.1.1; locus tags:  
425 COMBST215\_v1\_20566; 40196; 50105) and catalase enzymes (EC number:  
426 1.11.1.21; locus tag: COMBST215\_v1\_11754 and EC: 1.11.1.6; locus tags:  
427 COMBST215\_v1\_60157; 140122)). In comparison with other closely related strains,  
428 the new strain BS-T2-15<sup>T</sup> is the only one with the genetic potential to achieve the

429 biosynthesis of betaxanthin (a secondary metabolite) and to degrade alanine and  
430 anthranilate (Table S9).

431 In conclusion, from the clear genotypic distance with the closest genera, the  
432 physiological similarities and some phenotypical and chemotaxonomic differences,  
433 we comply with the phylo-phenetic concept that currently prevails for the description  
434 of a new genus. Thus, we assigned strain BS-T2-15<sup>T</sup> to a novel species, of a novel  
435 genus, for which the name *Scleromatobacter humisilvae* gen. nov., sp. nov. is  
436 proposed.

437

#### 438 **DESCRIPTION OF *SCLEROMATOBACTER* GEN. NOV.**

439 *Scleromatobacter* sp. (scl.ro'mae. N.L. gen. n. scleromae, of scleroma, a hardened  
440 part; derived from the colonies that are incrustated in solid medium when the strain  
441 grows in Petri dishes).

442 Cells are Gram-negative, mesophilic, aerobic, chemoorganotrophic, straight rod-  
443 shaped (0.6 to 0.9 µm by 1.7 to 2.7 µm in size) and motile with presence of storage  
444 granules. Oxidase-negative and catalase-positive. The predominant fatty acids are  
445 C<sub>16:1</sub> ω7c, C<sub>16:0</sub> and C<sub>14:0</sub> 2-OH. The polar lipid profile consists of a mixture of  
446 phosphatidylethanolamine, diphosphatidylglycerol and phosphatidylglycerol and the  
447 main ubiquinone is Q-8. The estimated size of the genome is 6.28 Mb with a DNA  
448 G+C content of 69.56 mol%. Phylogenetically, on the base of whole genome  
449 comparisons, the genus belongs to the family *Comamonadaceae*, order  
450 *Burkholderiales*. Overall, the genus belongs to the *Rubrivivax-Roseateles-Leptothrix-*  
451 *Azohydromonas-Aquicola-Ideonella* branch. The type species is *Scleromatobacter*  
452 *humisilvae* (BS-T2-15<sup>T</sup>).

453

454 **DESCRIPTION OF *SCLEROMATOBACTER HUMISILVAE* GEN. NOV. SP. NOV.**

455 *Scleromatobacter humisilvae* (hu.mi.sil'vae. L. fem. n. *humus*, soil; L. fem. n. *silva*,  
456 forest; N.L. gen. fem. n. *humisilvae*; from forest soil; from the forest soil where the  
457 strain has been isolated).

458 Displays the following properties in addition to those given in the genus description:

459 Colonies are circular, rough and incrustated in the agar medium with a color between  
460 white and ivory. Optimal growth occurs at 20-22°C, pH 6 and 0% NaCl. Positive for  
461 nitrate reduction. Does not respire chlorate. The following carbon sources are used:  
462 L-arabinose, D-cellobiose, D-glucose, D-ribose, D-arabitol, adonitol, butyrate,  
463 gluconate, pyruvate, L-leucine, L-proline, N-acetylglucosamine, p-hydroxy  
464 phenylacetic acid, bromo succinic acid, L-pyroglutamic acid, tween 40 and 80,  
465 uridine, putrescine and dextrine. On the contrary, unable to use: citrate, acetate,  
466 aspartate, benzoate, formate, methyl-pyruvate, mono-methyl-succinate, cis-aconitic  
467 acid, D-galactonic acid lactone, D-galacturonic acid, D-gluconic acid, D-glucosaminic  
468 acid, D-glucuronic acid,  $\alpha$ -,  $\beta$ -,  $\gamma$ -hydroxy butyric acid, p-hydroxyphenylacetic acid,  
469 itaconic acid,  $\alpha$ -keto butyric acid,  $\alpha$ -keto glutaric acid,  $\alpha$ -keto valeric acid, D,L-lactic  
470 acid, malonic acid, propionic acid, quinic acid, D-saccharic acid, sebacic acid,  
471 succinic acid, succinamic acid, L-aspartic acid, L-glutamic acid, glycyl-L-Aspartic  
472 acid, glycyl-L-glutamic acid, L-pyroglutamic acid,  $\gamma$ -amino butyric acid, urocanic acid,  
473 phosphate, glucose-1-phosphate, glucose-2-phosphate, D-fructose, L-fucose, D-  
474 galactose, D-galactose, gentiobiose, CM-cellulose, D-psicose, D-raffinose, L-  
475 rhamnose, sucrose, D-maltose, D-trehalose, turanose, D-mannose, D-melibiose,  $\alpha$ -  
476 D-lactose, lactulose, maltose,  $\beta$ -methyl-D-glucoside, m-inositol, xylitol, D-mannitol, i-  
477 erythritol, D-sorbitol, glycerol, D,L- $\alpha$ -glycerol, 2,3-butanediol, N-acetyl-D-  
478 glucosamine, N-acetyl-D-galactosamine, 2-aminoethanol, phenylethylamine,

479 Glucuronamide, L-alaninamide, D-, L-alanine, L-phenylalanine, L-alanyl-glycine, L-  
480 asparagine, L-histidine, L-ornithine, hydroxy-L-proline, D-, L-serine, L-threonine, D,L-  
481 carnitine, thymidine,  $\alpha$ -cyclodextrin, inosine, glycogen, xylan, lignin and chitin.  
482 Produces the  $\alpha$ -glucosidase but is negative for urease.

483

484 The type strain BS-T2-15<sup>T</sup> (DSM 113115<sup>T</sup> =UBOCC-M-3373<sup>T</sup>) was isolated from bulk  
485 soil in direct contact with decaying oak placed for 9 months on the floor of the  
486 Champenoux forest experimental site (France). The 16S rRNA gene sequence and  
487 the assembled genome sequences of strain BS-T2-15<sup>T</sup> have been deposited in  
488 GenBank under the accession numbers OM630150 and JAJLJH000000000,  
489 respectively.

490

#### 491 **Acknowledgements**

492 We are grateful to Claire Geslin (UBO, LM2E) and Philippe Eliès (UBO, Plateforme  
493 d'imagerie et de mesures en microscopie (PIMM)) for their technical assistance in  
494 TEM imaging. We acknowledge Nadège Bienvenu (UBO, LM2E) for her help  
495 concerning the deposit of the strain at the UBOCC. We thank Erwann Vince and  
496 Xavier Philippon for their technical help concerning ionic chromatography. The  
497 LABGeM (CEA/Genoscope & CNRS UMR8030), the France Génomique and French  
498 Bioinformatics Institute national infrastructures (funded as part of Investissement  
499 d'Avenir program managed by Agence Nationale pour la Recherche, contracts ANR-  
500 10-INBS-09 and ANR-11-INBS-0013) are acknowledged for support within the  
501 MicroScope annotation platform. The UMR1136 is supported by the ANR through the  
502 Labex Arbre (ANR-11-LABX-0002-01).

503

504 **Funding information**

505 This research was funded by the Sino-French IRP 1211 MicrobSea to K.A. and by  
506 the UMR6197.

507

508 **Conflict of interest**

509 The authors declare that there are no conflicts of interest.

510

511 **References**

- 512 1. **Ulyshen MD.** Wood decomposition as influenced by invertebrates. *Biol Rev* 2016;  
513 91:70–85.
- 514 2. **Tláskal V, Brabcová V, Větrovský T, Jomura M, López-Mondéjar R, et al.**  
515 Complementary roles of wood-inhabiting fungi and bacteria facilitate deadwood  
516 decomposition. *Msystems* 2021; 6:e01078–20.
- 517 3. **Johnston SR., Boddy L, Weightman AJ.** Bacteria in decomposing wood and  
518 their interactions with wood-decay fungi. *FEMS Microbiol. Ecol.* 2016; 92(11).
- 519 4. **Mieszkin S, Richet P, Bach C, Lambrot C, Augusto L, et al.** Oak decaying  
520 wood harbors taxonomically and functionally different bacterial communities in  
521 sapwood and heartwood. *Soil Biol Biochem* 2021; 155:108160.
- 522 5. **Liu Y, Du J, Pei T, Du H, Feng GD, et al.** Genome-based taxonomic  
523 classification of the closest-to-*Comamonadaceae* group supports a new family  
524 *Sphaerotilaceae* fam. nov. and taxonomic revisions. *Syst Appl Microbiol* 2022;  
525 45:126352.
- 526 6. **Bedics A, Táncsics A, Tóth E, Banerjee S, Harkai P, et al.** Microaerobic  
527 enrichment of benzene-degrading bacteria and description of *Ideonella*  
528 *benzenivorans* sp. nov., capable of degrading benzene, toluene and  
529 ethylbenzene under microaerobic conditions. *Antonie von Leeuwenhoek* 2022;  
530 115: 1113-1128.
- 531 7. **Lechner U, Brodkorb D, Geyer R, Hause G, Härtig C et al.** *Aquicola*  
532 *tertiaricarbonis* gen. nov., sp. nov., a tertiary butyl moiety-degrading bacterium. *Int*  
533 *J Syst Evol Microbiol* 2007; 57 :1295–1303.
- 534 8. **Malmqvist Å, Welander T, Moore E, Ternström A, Molin G et al.** *Ideonella*  
535 *dechloratans* gen. nov., sp. nov., a new bacterium capable of growing  
536 anaerobically with chlorate as an electron acceptor. *Syst Appl Microbiol* 1994;  
537 17:58–64.
- 538 9. **Mieszkin S, Pouder E, Uroz S, Simon-Colin C, Alain K.** *Acidisoma silvae* sp.  
539 nov. and *Acidisoma cellulositytica* sp. nov., two acidophilic bacteria isolated from  
540 decaying wood, hydrolyzing cellulose and producing poly-3-hydroxybutyrate.  
541 *Microorganisms* 2021; 9:2053.
- 542 10. **Tindall BJ.** A comparative study of the lipid composition of *Halobacterium*  
543 *saccharovororum* from various sources. *Syst Appl Microbiol* 1990;13:128–130.
- 544 11. **Tindall BJ.** Lipid composition of *Halobacterium lacus profundus*. *FEMS Microbiol*  
545 *Lett* 1990; 66: 199–202.

- 546 12. **Kuykendall LD, Roy MA, O'Neill JJ, Devine TE.** Fatty acids, antibiotic  
547 resistance, and deoxyribonucleic acid homology groups of *Bradyrhizobium*  
548 *japonicum*. *Int J Syst Bact* 1988; 38:358–361.
- 549 13. **Jeon CO., Park W, Ghiorse WC, Madsen EL.** *Polaromonas naphthalenivorans*  
550 sp. nov., a naphthalene-degrading bacterium from naphthalene-contaminated  
551 sediment. *Int J Syst Evol Microbiol* 2004; 54:93–97.
- 552 14. **Blümel S, Busse H J, Stolz A, Kämpfer P.** *Xenophilus azovorans* gen. nov., sp.  
553 nov., a soil bacterium that is able to degrade azo dyes of the Orange II type. *Int J*  
554 *Syst Evol Microbiol* 2001; 51:1831–1837.
- 555 15. **Chen WM, Chen LC, Sheu DS, Tsai JM, Sheu SY.** *Ideonella livida* sp. nov.,  
556 isolated from a freshwater lake. *Int J of Syst Evol Microbiol* 2020;70:4942–4950.
- 557 16. **Sheu SY, Hsieh TY, Chen WM.** *Aquincola rivuli* sp. nov., isolated from a  
558 freshwater stream. *Int J Syst Evol Microbiol* 2019; 69:2226–2232.
- 559 17. **Spring S, Kämpfer P, Ludwig W, Schleifer KH.** Polyphasic characterization of  
560 the genus *Leptothrix*: new descriptions of *Leptothrix mobilis* sp. nov. and  
561 *Leptothrix discophora* sp. nov. nom. rev. and emended description of *Leptothrix*  
562 *cholodnii* emend. *Syst Appl Microbiol* 1996; 19:634–643.
- 563 18. **Willems A, Gillis M, De Ley J.** Transfer of *Rhodocyclus gelatinosus* to  
564 *Rubrivivax gelatinosus* gen. nov., comb. nov., and phylogenetic relationships with  
565 *Leptothrix*, *Sphaerotilus natans*, *Pseudomonas saccharophila*, and *Alcaligenes*  
566 *latus*. *Int J Syst Evol Microbiol* 1991; 41:65–73.
- 567 19. **Seemann T, Booth T.** BARNAP: BAasic Rapid Ribosomal RNA Predictor  
568 [Internet]. 2020; Berlin: GitHub; 2013. p.
- 569 20. **Yoon SH, Ha SM, Kwon S, Lim J, Kim Y.** Introducing EzBioCloud: a  
570 taxonomically united database of 16S rRNA gene sequences and whole-genome  
571 assemblies. *Int J Syst Evol Microbiol* 2017; 67:1613.
- 572 21. **Gouy M, Guindon S, Gascuel O.** SeaView version 4: A multiplatform graphical  
573 user interface for sequence alignment and phylogenetic tree building. *Mol Biol*  
574 *Evol* 2010; 27:221–224
- 575 22. **Saitou N, Nei, M.** The neighbor-joining method: A new method for reconstructing  
576 phylogenetic trees. *Mol Biol Evol* 1987; 4:406–425.
- 577 23. **Kimura M.** The Neutral Theory of Molecular Evolution. Cambridge: Cambridge  
578 University Press; 1983.
- 579 24. **Dereeper A, Guignon V, Blanc G, Audic S, Buffet S, et al.** Phylogeny. fr: robust  
580 phylogenetic analysis for the non-specialist. *Nucleic Acids Res* 2008; 36: W465-  
581 W469.
- 582 25. **Guindon S, Dufayard JF, Lefort V, Anisimova M, Hordijk W, et al.** New  
583 algorithms and methods to estimate maximum-likelihood phylogenies: assessing  
584 the performance of PhyML 3.0. *Syst Biol* 2010; 59:307-321.
- 585 26. **Charbonnier F, Forterre P, Erauso G, Prieur D.** Purification of plasmids from  
586 thermophilic and hyperthermophilic archaeobacteria. In *Archaea: A Laboratory*  
587 *Manual*; Robb, F.T., Place, A.R., DasSarma, S., Schreier, H.J., Fleischmann,  
588 E.M., Eds.; Cold Spring Harbor Laboratory Press: Woodbury, NY, USA, 1995; pp.  
589 87–90.
- 590 27. **Andrews, S.** FastQC: A quality control tool for high throughput sequence data.  
591 2010.
- 592 28. **Bankevich A, Nurk S, Antipov D, Gurevich AA, Dvorkin M.** SPAdes: a new  
593 genome assembly algorithm and its applications to single-cell sequencing. *J*  
594 *Comput Biol* 2012; 19:455–477.

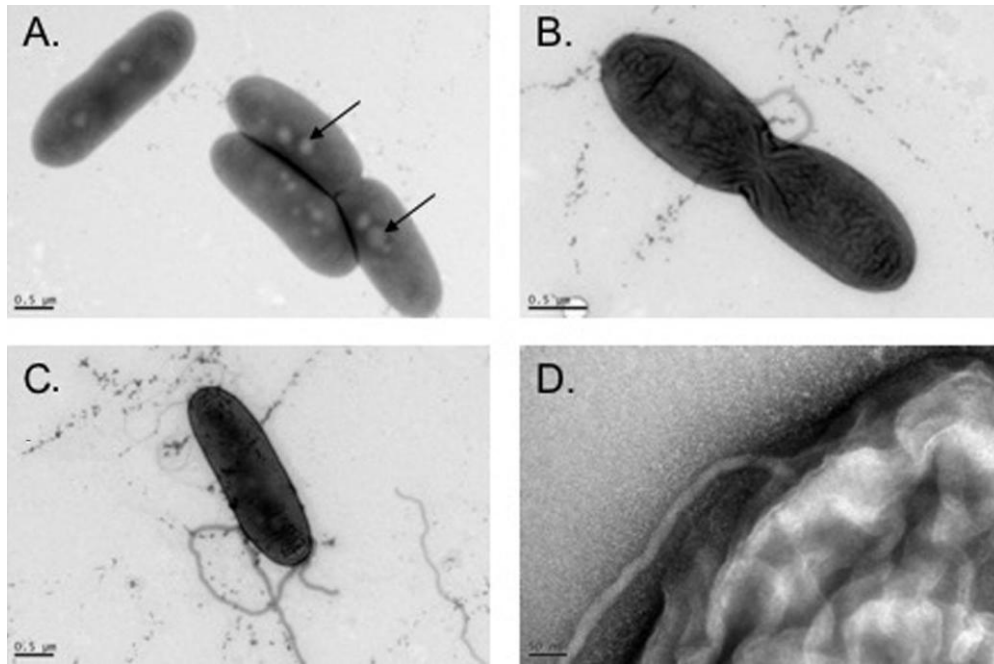


- 595 29. **Vallenet D, Calteau A, Dubois M, Amours P, Bazin, A. et al.** MicroScope: an  
596 integrated platform for the annotation and exploration of microbial gene functions  
597 through genomic, pangenomic and metabolic comparative analysis. *Nucleic Acids*  
598 *Res* 2020; 48(D1):D579-D589.
- 599 30. **Alteio LV, Schulz F, Seshadri R, Varghese N, Rodriguez-Reillo W, et al.**  
600 Complementary metagenomic approaches improve reconstruction of microbial  
601 diversity in a forest soil. *msystems* 2020; 5:e00768-19.
- 602 31. **Martin G, Rissanen AJ, Garcia SL, Mehrshad M, Buck M, et al.** Candidatus  
603 *Methylumidiphilus* drives peaks in methanotrophic relative abundance in stratified  
604 lakes and ponds across Northern landscapes. *Front Microbiol* 2021; 12:669937.
- 605 32. **Garcia SL, Mehrshad M, Buck M, Tsuji JM, Neufeld JD, et al.** Freshwater  
606 Chlorobia exhibit metabolic specialization among cosmopolitan and endemic  
607 populations. *msystems* 2021; 6:e01196-20.
- 608 33. **Rissanen AJ, Saarela T, Jäntti H, Buck M, Peura S, et al.** Vertical stratification  
609 patterns of methanotrophs and their genetic controllers in water columns of  
610 oxygen-stratified boreal lakes. *FEMS Microbiol Ecol* 2021; 97:fiaa252.
- 611 34. **Eren AM, Kiefl E, Shaiber A, Veseli I, Miller S et al.** Community-led, integrated,  
612 reproducible multi-omics with anvio. *Nat Microbiol* 2021; 6:3–6.
- 613 35. **Hoang DT, Chernomor O, von Haeseler A, Minh BQ, Vinh LS.** UFBoot2:  
614 improving the ultrafast bootstrap approximation. *Mol Biol Evol* 2018; 35:518–522.
- 615 36. **Minh BQ, Schmidt HA, Chernomor O, Schrempf D, Woodhams MD, et al.** IQ-  
616 TREE 2: new models and efficient methods for phylogenetic inference in the  
617 genomic era. *Mol Biol Evol* 2020; 37:1530–1534.
- 618 37. **Chaumeil PA, Mussig AJ, Hugenholtz P, Parks DH.** GTDB-Tk: a toolkit to  
619 classify genomes with the Genome Taxonomy Database. *Bioinform* 2020; 6:1925-  
620 1927.
- 621 38. **Chaumeil PA, Mussig AJ, Hugenholtz P, Parks DH, et al.** GTDB-Tk v2:  
622 memory friendly classification with the Genome Taxonomy Database. *bioRxiv*  
623 2022.
- 624 39. **Jain C, Rodriguez-R LM, Phillippy AM, Konstantinidis KT, Aluru S.** High  
625 throughput ANI analysis of 90K prokaryotic genomes reveals clear species  
626 boundaries. *Nat Commun* 2018; 9:1-8.
- 627 40. **Meier-Kolthoff JP, Auch AF, Klenk HP, Göker M.** Genome sequence-based  
628 species delimitation with confidence intervals and improved distance functions.  
629 *BMC Bioinform* 2013; 14:60.
- 630 41. **Kim D, Park S, Chun J.** Introducing EzAAI: a pipeline for high throughput  
631 calculations of prokaryotic average amino acid identity. *J Microbiol* 2021; 59:476-  
632 480.
- 633 42. **Qin QL, Xie BB, Zhang XY, Chen XL, Zhou BC, et al.** A proposed genus  
634 boundary for the prokaryotes based on genomic insights. *J Bacteriol* 2014 ;  
635 196:2210-2215.
- 636 43. **Richter M, Rosselló-Móra R.** Shifting the genomic gold standard for the  
637 prokaryotic species definition. *Proc Natl Acad Sci USA* 2009; 106:19126–19131.
- 638 44. **Wayne L, Brenner DJ, Colwell RR, Grimont PAD, Kandler O et al.** Report of  
639 the Ad Hoc Committee on Reconciliation of Approaches to Bacterial Systematics.  
640 *Int J Syst Bacteriol* 1987; 37:463–464.
- 641 45. **Konstantinidis KT, Rosselló-Móra R, Amann R.** Uncultivated microbes in need  
642 of their own taxonomy. *ISME J* 2017; 11:2399-2406.

643 46. **Barco RA, Garrity GM, Scott JJ, Amend JP, Nealson KH et al.** A genus  
644 definition for bacteria and archaea based on a standard genome relatedness  
645 index. *mBio* 2020; 11:e02475–19.  
646

647  
648

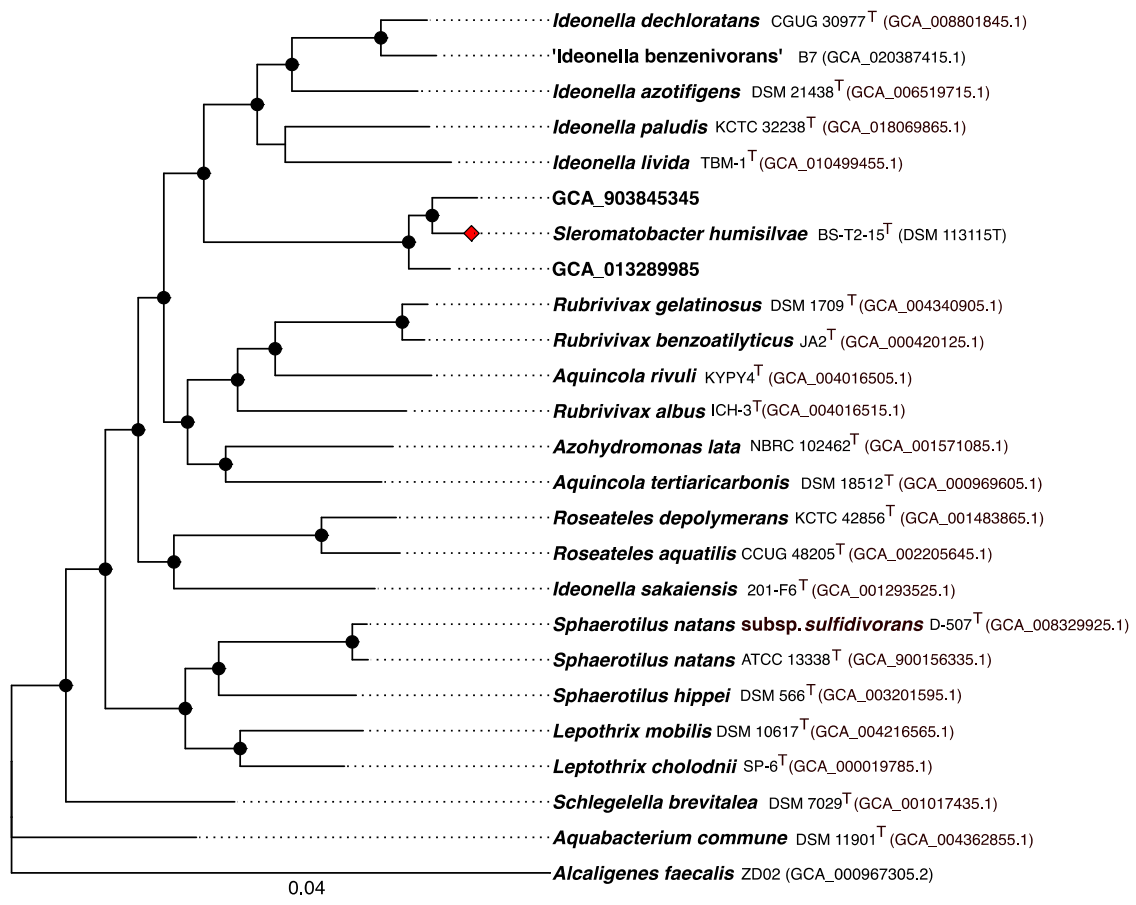
**List of figures:**



649

650  
651  
652  
653

**Figure 1. Transmission electron micrographs of cells of strain BS-T2-15<sup>T</sup> showing (A) intracellular granules (indicated by black arrows), (B) a dividing cell (by binary fission), (C) a cell with its polar flagellum, and (D) the insertion point of the flagellum.**



654  
655 **Fig. 2.** Phylogenomic tree (concatenated alignment of 340 shared gene clusters) showing  
656 the phylogenomic position of strain BS-T2-15<sup>T</sup>, its two closely related MAGs and  
657 representatives of other related taxa. The tree was built using IQ-Tree and the maximum  
658 likelihood method with 1,000 replicates for the calculation of the ultrafast bootstrap. Bootstrap  
659 values >95% are indicated at branching point by a dot. The tree was rooted using  
660 *Alcaligenes faecalis* ZD02 (GCA\_000967305.2) as the outgroup. Bar, 0.04 substitutions per  
661 position.

662 **List of tables:**

663

664 **Table 1. Differential characteristics of strain BS-T2-15<sup>T</sup> and type strains of**  
 665 **closely related genera.**

666 Taxa : 1. BS-T2-15<sup>T</sup>, 2. *Leptothrix mobilis* DSM 10617<sup>T</sup>, 3. *Rubrivivax gelatinosus* DSM  
 667 1709<sup>T</sup>, 4. *Ideonella dechloratans* CGUG 30977<sup>T</sup>, 5. *Aquincola tertiaricarbonis* DSM 18512<sup>T</sup>.

668 Data are from Mieszkin *et al.* [4], Lechner *et al.* [7], Malmqvist *et al.* [8], Chen *et al.* [15],  
 669 Sheu *et al.* [16], Spring *et al.* [17] and Willems *et al.* [18]. +, Positive; –, negative; NA, not  
 670 available; w, weak growth; <sup>a</sup>Summed feature 3 comprises C16: 1  $\omega$ 7c and/or C16: 1  $\omega$ 6c. All  
 671 strains are motile, positive for tween 40 hydrolysis, and negative for urease activity and  
 672 citrate utilization. <sup>s</sup>As all strains have not been grown under exactly the same conditions nor  
 673 in the same media, percentages of fatty acids cannot be compared from one strain to  
 674 another.

675

Characteristics	1	2	3	4	5
<b>Colony color</b>	White-ivory	Dark-brown	Orange-brown	White	White
<b>Cell size (<math>\mu</math>m)</b>	0.6-0.9 x 1.7-2.7	0.6-0.8 x 1.5-12	0.4-0.7 x 1-3	0.7-1 x 2.5-5	0.8-1.1 x 1.2-2.3
<b>Temperature range (optimum) (<math>^{\circ}</math>C)</b>	4-30 (20-22)	10-37	10-45 (37-40)	15-30 (30)	4-40 (30)
<b>pH growth range (optimum)</b>	2-12 (6)	6.5-8.5	5-9 (6-7)	6-8 (6-7)	5-9 (6-7)
<b>NaCl tolerance (optimum) (% w/v)</b>	0-0.5 (0)	NA	0-2 (1)	0-2	0-1 (0)
<b>Carbon sources utilization</b>					
Acetate	–	–	+	+	+
Butyrate	+	–	+	+	+
Gluconate	W	–	NA	–	+
Pyruvate	+	–	+	+	+
Arabinose	+	NA	–	–	NA
Cellobiose	+	NA	–	–	NA
CM-cellulose	-	NA	–	+	–
D-Glucose	+	–	–	+	+
D-Maltose	–	–	+	–	+
D-Mannose	–	–	–	+	+
D-Mannitol	–	+/-	–	–	+
<i>N</i> -Acetylglucosamine	W	–	–	–	+
<b>Indole formation</b>	–	–	+	–	–
<b>Enzymatic activities</b>					
Catalase	+	NA	–	+	+
Oxidase	–	+	+	+	+
Nitrate reductase	+	NA	+	+	–
$\alpha$ -Glucosidase	+	NA	–	–	+
<b>Quinone type</b>	Q-8	Q-8	Q-8, MK-8	Q-8	Q-8
<b>Polar lipids</b>					
Diphosphatidylglycerol (DPG)	+	–	+	+	+
<b>Major fatty acids (%)<sup>s</sup></b>					
14: 0 2-OH	10.49	–	–	–	–
16: 1 <i>cis</i> -9	–	53.04	–	–	39
16: 1 $\omega$ 7c	40.45	–	–	–	–
Summed feature 3 <sup>a</sup>	–	–	42.8	40.2	–
<b>DNA G+C content (mol%)</b>	69.6	68	71.9	68.1	70.5
<b>Isolation source</b>	Forest	Freshwater	Acetate	Activated	Aquifer

676 **Table 2. Comparison of whole-cell fatty acid profiles (% of the total) of strain**  
 677 **BS-T2-15<sup>T</sup> with type strains of closely related genera.**

678 Taxa : 1. BS-T2-15<sup>T</sup>, 2. *Leptothrix mobilis* DSM 10617<sup>T</sup>, 3. *Rubrivivax gelatinosus* DSM  
 679 1709<sup>T</sup>, 4. *Ideonella dechloratans* CGUG 30977<sup>T</sup>, 5. *Aquincola tertiaricarbonis* DSM 18512<sup>T</sup>.  
 680 Values are percentages of the fatty acids that were assigned to fatty acids in the peak-  
 681 naming table of the MIS database (MIDI, Microbial ID, Newark, DE 19711 U.S.A.). The  
 682 nomenclature is as follows: the first number indicates the number of carbon atoms in the  
 683 molecule; 'OH' and 'cyclo' indicate hydroxy or cyclic fatty acids; the second number following  
 684 the colon indicates the number of double bonds present. The position of the double bond is  
 685 indicated by the carbon atom position starting from the methyl ( $\omega$ ) end of the molecule. *c*, cis  
 686 isomer. Data are from Lechner *et al.* [7], Malmqvist *et al.* [8], Sheu *et al.* [16] and Spring *et al.*  
 687 [18]. Major fatty acids (>10% of the total fatty acids) are indicated in bold.

Fatty acids	1	2	3	4	5
10: 0 3-OH	5.99	4.54	4.8	2.4	2
12: 0	–	2.43	3.7	2.1	4
12: 0 2-OH	0.47	–	–	2.5	–
12: 0 3-OH	3.17	–	–	4.1	–
14: 0	3.14	0.77	5.4	1.5	2
14: 0 2-OH	<b>10.49</b>	–	–	–	–
15: 0	–	–	–	–	3
15: 1	–	–	–	–	2
15: 1 $\omega$ 6 <i>c</i>	–	–	1.7	–	–
16: 0	<b>25.18</b>	<b>30.29</b>	<b>33.1</b>	<b>31.5</b>	<b>37</b>
16: 1 <i>cis</i> -9	–	<b>53.04</b>	–	–	<b>39</b>
16: 1 $\omega$ 7 <i>c</i>	<b>40.45</b>	–	–	–	–
17: 0	–	–	1.1	–	2
17: 0 cyclo	–	–	–	–	2
17: 0 cyclo $\omega$ 7 <i>c</i>	1.44	–	–	–	–
18: 0	–	1.19	–	–	1
18: 1	–	–	–	–	6
18: 1 <i>cis</i> -9,11 <sup>a</sup>	–	6.99	–	–	–
18: 1 $\omega$ 7 <i>c</i>	9.68	–	4.5	<b>12.7</b>	–
19: 1 <i>cis</i> -9,10 <sup>b</sup>	–	0.84	–	–	–
Summed feature	–	–	<b>42.8</b>	<b>40.2</b>	–

3<sup>c</sup>

688 –, Not detected

689 <sup>a</sup>Sum of both compounds: cis-9octadecenoic acid and cis-11-octadecenoic acid690 <sup>b</sup>cis-9,10-methyleneoctadecanoic acid691 <sup>c</sup>Summed feature 3 comprises C16: 1  $\omega$ 7*c* o and/or C16: 1  $\omega$ 6*c*

692

693 **Table 3. Genome statistics and overall genome relatedness indices (OGRI) between**  
694 **strain BS-T2-15<sup>T</sup> and type strains of closely related genera and closely related MAGs.**  
695 Taxa : 1. BS-T2-15<sup>T</sup>, 2. *Leptothrix mobilis* DSM 10617<sup>T</sup>, 3. *Rubrivivax gelatinosus* DSM  
696 1709<sup>T</sup>, 4. *Ideonella dechloratans* CGUG 30977<sup>T</sup>, 5. *Aquicola tertiaricarbonis* DSM 18512<sup>T</sup>.  
697 6. *Azohydromonas lata* NBRC 102462<sup>T</sup>, 7. *Roseateles depolymerans* KCTC 42856<sup>T</sup>, 8.  
698 MAG GCA\_013289985.1, 9. MAG\_GCA\_903845345.1.

	1	2	3	4	5	6	7	8	9
<b>Number of contigs</b>	28	17	36	158	98	342	1	210	631
<b>Size (Mb)</b>	6.27	4.65	5.08	4.51	6.32	7.18	5.68	6	5.4
<b>GC content (%)</b>	69.56	69.00	71.40	69.30	70.20	69.00	66.60	69.55	69.50
<b>Number of CDS</b>	5,712	4,019	4,691	4,172	5,711	6,349	4,894	5,441	5,362
<b>rRNA</b>	3	6	3	7	3	4	12	3	1
<b>tRNA</b>	55	49	46	59	43	46	58	19	17
<b>dDDH (%)</b>	100	20.50	20.40	20.10	20.30	20.30	20.00	30.10	33.40
<b>ANI (%)</b>	100	79.50	79.70	79.70	79.60	78.60	78.50	87.80	88.90
<b>AAI (%)</b>	100	65.34	66.03	66.57	65.48	65.32	64.27	84.14	86.43
<b>POCP (%)</b>	100	43.17	44.84	47.33	49.02	40.89	49.27	72.60	74.76
<b>AF</b>	1.0	0.42	0.48	0.43	0.40	0.32	0.29	0.71	0.80

699